NASA Contractor Report 181802

On the Relationship Between Matched Filter Theory as Applied to Gust Loads and Phased Design Loads Analysis

Thomas A. Zeiler and Anthony S. Pototzky
Planning Research Corporation
Hampton, VA 23666

Contract NAS1-18000

APRIL 1989

National Aeronautics and
Space Administration

Langley Research Center
Hampton, Virginia 23665

On the Relationship Between Matched Filter Theory as Applied to Gust Loads and Phased Design Loads Analysis

by

Thomas A. Zeiler and Anthony S. Pototzky
Planning Research Corporation
Aerospace Technologies Division
Hampton, Virginia

SUMMARY

This report gives a theoretical basis and example calculations that demonstrate the relationship between the Matched Filter Theory approach to the calculation of time-correlated gust loads and Phased Design Load Analysis in common use in the aerospace industry. The relationship depends upon the duality between Matched Filter Theory and Random Process Theory and upon the fact that Random Process Theory is used in Phased Design Loads Analysis in determining an equiprobable loads design ellipse. Extensive background information describing the relevant points of Phased Design Loads Analysis, calculating time-correlated gust loads with Matched Filter Theory, and the duality between Matched Filter Theory and Random Process Theory is given. It is then shown that the time histories of two time-correlated gust load responses, determined using the Matched Filter Theory approach, can be plotted as parametric functions of time and that the resulting plot, when superposed upon the design ellipse corresponding to the two loads, is tangent to the ellipse. The question is raised of whether or not it is possible for a parametric load plot to extend outside the associated design ellipse. If it is possible, then the use of the equiprobable loads design ellipse will not be a conservative design practice in some circumstances.

TABLE OF CONTENTS

INTRODUCTION

An aircraft structure must be designed to withstand the loads it is expected to encounter during its lifetime. In some cases the loading conditions can be modeled deterministically. Specific maneuvers, takeoff and landing, and pressurization cycles are examples. Atmospheric turbulence (gust loading), however, is a random process modeled statistically as a Gaussian process. Ideally, loads analysts would like to know the gust load distributions throughout the aircraft as specific functions of time so that proper combinations of loads can be analyzed. However, since only the statistical characteristics of the turbulence are known, as described by the gust velocity power spectral density function, only the likely combinations or phasing of loads can be determined. This is referred to as Phased Design Loads Analysis (PDLA).

The Statistical Discrete Gust (SDG) method had been developed [1] as a candidate method for analyzing aircraft for gust loads. The method determines worst-case gust loads and the corresponding critical gust profiles that produce the responses. Its potential advantages over Power Spectral Density (PSD) methods, such as PDLA, are that the loads it produces are time-correlated, and it is applicable to nonlinear systems. Its implementation involves an extensive search procedure that, although simplified for linear systems, can be time consuming.

During the course of a NASA evaluation of a claimed "overlap" between SDG and PSD methods, a new method for calculating maximum and time-correlated gust loads for linear systems was discovered [2]. The method is based upon a new way of interpreting the Matched Filter principle from radar theory and can obtain the maximum and time-correlated responses as well as the critical gust profiles through direct calculation instead of through a search. It was further found that there was a duality between the Matched Filter Theory (MFT) and Random Process Theory (RPT) results, upon which the PSD methods of gust analysis are based, so that identical results can be obtained directly through methods of RPT. This duality also allows a relationship to be established between MFT and PDLA. The present report describes this relationship by first outlining the pertinent aspects of PDLA and the MFT/RPT duality, and then giving the analytical basis for the relationship with some calculated examples.

BACKGROUND

Phased Design Loads Analysis and The Equiprobable Loads Design Ellipse

In Phased Design Loads Analysis (PDLA), the turbulence is assumed Gaussian and the vehicle structure is assumed linear. The response of the structure to the turbulence is then also Gaussian. Any two gust responses, y and z (e.g., bending moment and shear force at some wing station), are related by a bivariate or joint probability density function [3],

$$P(y,z) = \frac{\exp\left[-\frac{1}{2(1-\rho_{zy}^2)\sigma_g^2}\left(\frac{y^2}{\bar{A}_y^2} - 2\rho_{zy}\frac{y\,z}{\bar{A}_y\bar{A}_z} + \frac{z^2}{\bar{A}_z^2}\right)\right]}{2\pi\sigma_g^2\bar{A}_y\bar{A}_z(1-\rho_{zy}^2)^{1/2}} \tag{1}$$

where σ_g is the gust velocity root-mean-square (RMS), the $\bar{A}$'s are the ratios of the indicated response RMS to the gust RMS, and are given by

$$\bar{A}^2 = \frac{\sigma^2}{\sigma_g^2} = \left[\frac{\frac{1}{2\pi}\int_{-\infty}^{\infty}\Phi_g(\omega)\bar{H}^*(\omega)\bar{H}(\omega)\,d\omega}{\frac{1}{2\pi}\int_{-\infty}^{\infty}\Phi_g(\omega)\,d\omega} \right], \tag{2}$$

where $\Phi_g(\omega)$ is the von Karman spectrum and $\bar{H}(\omega)$ is the load frequency response function.

Note that the von Karman spectrum is defined to be consistent with the use of the 2π factor in the inverse Fourier transform. The correlation coefficient (to be defined later) between the two response quantities is ρ_{zy}. By assigning values to the probability density P(y,z), contours of constant joint probability density are defined in the y - z plane by the exponential argument and are in the shapes of ellipses. Thus, for a given P(y,z), all combinations of y and z lying on the associated ellipse have an equal probability of occurring. The ellipse is known as the "equiprobable loads design ellipse", or just "design ellipse", and is depicted in Figure 1. For incremental gust loads about a 1-G flight condition, the ellipse is centered at the 1-G load values. The ellipse is bounded by a rectangle, tangent to the ellipse at the circled points, whose sides are determined, for design envelope analysis, by

$$Y_{design} = Y_{1-G} \pm U_\sigma \bar{A}_y \tag{3a}$$

$$Z_{design} = Z_{1-G} \pm U_\sigma \bar{A}_z\,, \tag{3b}$$

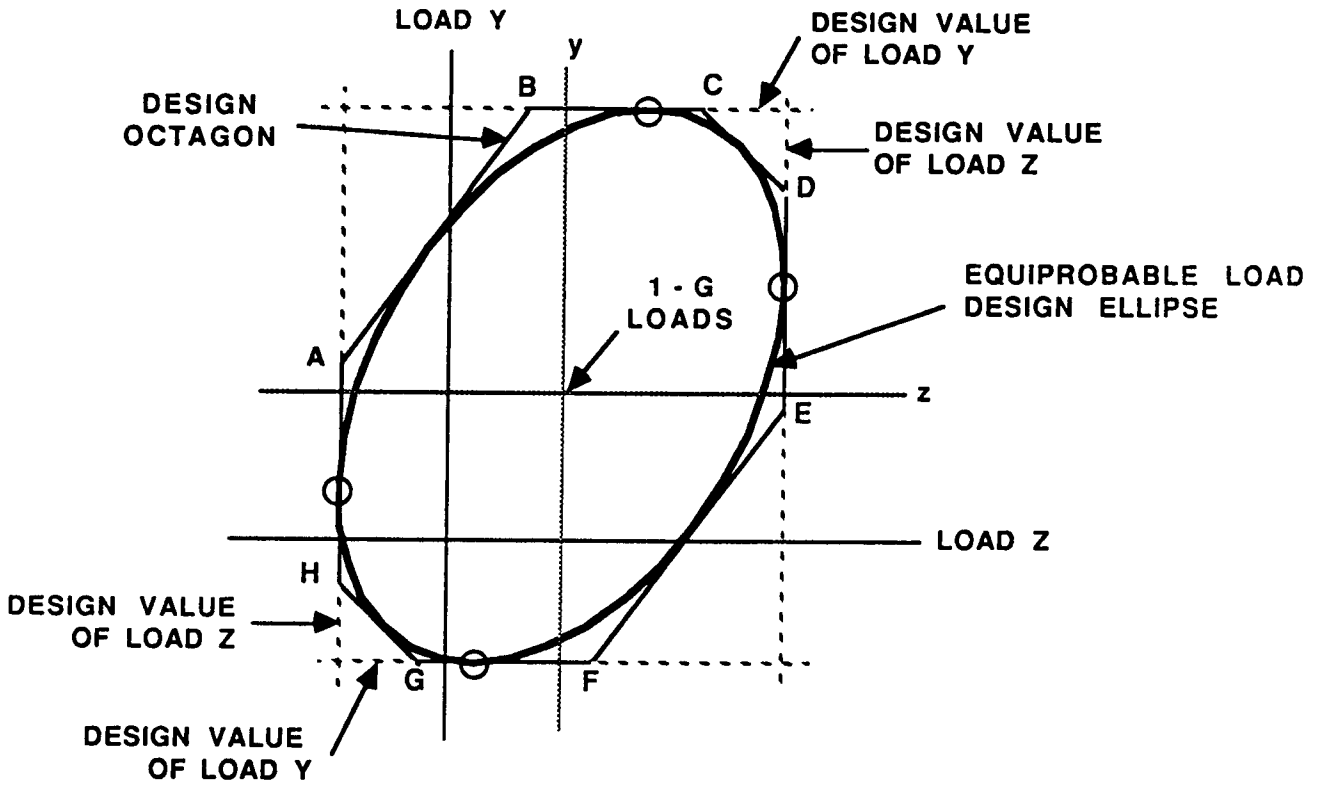

Figure 1. Equiprobable Loads Design Ellipse

where U_σ is the design gust velocity. The value of P(y,z) is chosen to correspond to the desired U_σ [4]. Since every possible design load combination (of which there are an infinite number) cannot be checked, the ellipse is circumscribed by a "design octagon" and the load combinations defined by the corner points (A, B, C, D, E, F, G, and H) are checked and are assumed to provide conservative values for the design stresses. An excellent summary of this and other aspects of current practices in designing for gust loads is given by Moon in Reference 4.

Normalized Design Ellipse

The equation for the ellipse can be written in terms of normalized loads as [5],

$$\psi^2 - 2\rho_{zy}\psi\zeta + \zeta^2 = (1 - \rho_{zy}^2) , \qquad (4)$$

where $\psi = y/(U_\sigma \bar{A}_y)$ and $\zeta = z/(U_\sigma \bar{A}_z)$ are the normalized load coordinates. The normalized ellipse, shown in Figure 2, is bounded by a square that is tangent to the ellipse at the circled points with sides at $\psi = \pm 1$ and $\zeta = \pm 1$. The correlation coefficient is defined,

$$\rho_{zy} = \frac{1}{2\pi} \int_{-\infty}^{\infty} \frac{\left(\Phi_g(\omega)/\sigma_g^2\right)}{\bar{A}_z \bar{A}_y} \left[\mathrm{Re}(\bar{H}_z(\omega))\, \mathrm{Re}(\bar{H}_y(\omega)) + \mathrm{Im}(\bar{H}_z(\omega))\, \mathrm{Im}(\bar{H}_y(\omega)) \right] d\omega . \qquad (5)$$

The correlation coefficient may assume a value between +1 and -1. When its magnitude is unity, the ellipse collapses to a straight line and indicates that the two loads are completely correlated. The maximum magnitudes of both occur together. If the magnitude of the correlation coefficient is zero, the ellipse becomes a circle and indicates that the loads are uncorrelated. The maximum magnitude of one occurs when the other is zero. As before, the ellipse is bounded by a design octagon. When the value of one of the normalized loads is at its maximum value of unity, the value of the other is equal to ρ_{zy}. This normalization is convenient since it eliminates dependence upon the actual gust intensity or the particular design gust velocity. Such factors can be applied to the normalized phased loads to obtain load magnitudes for further analyses.

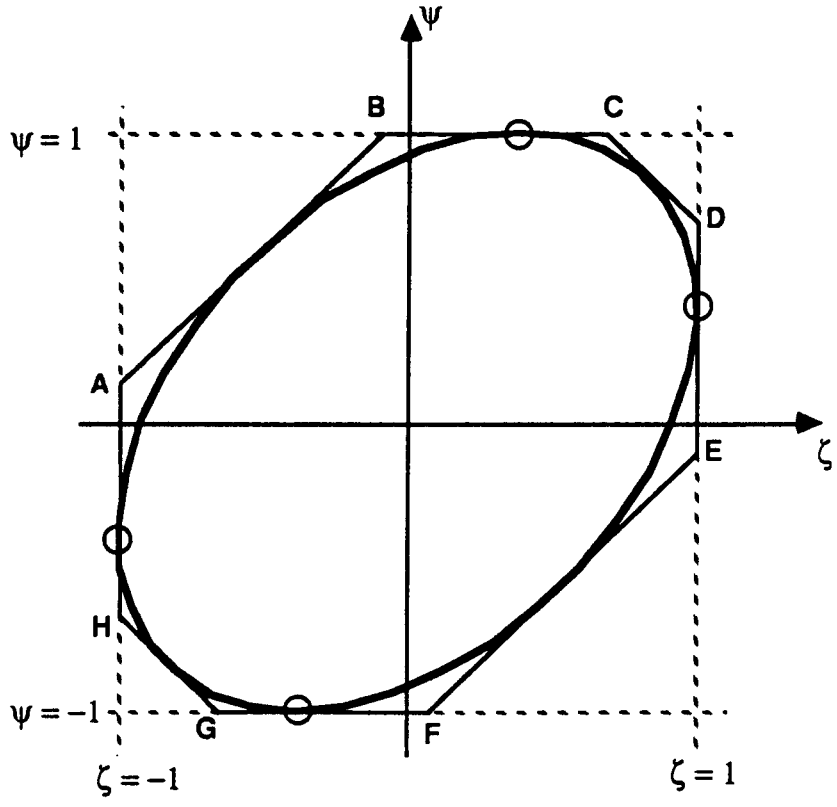

Figure 2. Normalized Equiprobable Loads Design Ellipse

Matched Filter Theory Approach to Gust Loads Analysis

The original objective of Matched Filter Theory (MFT) was the design of an electronic filter such that its response to a known input signal was maximum at a specific time [6]. The matched filter is designed so that its unit impulse response is proportional to the known excitation, shifted and reversed in time,

$$h_y(t) = Kx_y(-t + t_o), \tag{6a}$$

where K is an arbitrary constant, t_o is the time shift (also the time at which the response to $x_y(t)$ will be maximum), and $x_y(t)$ is the known excitation. The above simple relation can be inverted,

$$x_y(t) = \frac{1}{K} h_y(-t + t_o), \tag{6b}$$

to give the excitation that will maximize the response of a filter of known dynamics, characterized by $h_y(t)$, at time t_o.

In the MFT approach to gust load calculations [2] one considers the combined turbulence/aeroelastic system to be the known filter (as shown in Figure 3). Taking the constant, K, to be the root-mean-square (RMS), σ_{h_y}, of the unit impulse response of the filter results in a constraint that the excitation waveform, $x_y(t)$, have an RMS of unity. The waveform contains some spectral information that, when passed through the turbulence part of the combined turbulence/aeroelastic system "filter", produces the critical gust profile. The response of output quantity y is (from Ref. 2),

$$y_y(t) = \frac{\sigma_{h_y}}{2\pi} \int_{-\infty}^{\infty} X_y^*(\omega) X_y^*(\omega)\, e^{i\omega(t - t_o)}\, d\omega, \tag{7}$$

whose maximum is

$$\left| y_y(t) \right|_{max} = \left| y_y(t_o) \right| = \sigma_{h_y}. \tag{8}$$

The response of some other output quantity, z, to the excitation $x_y(t)$ (said to be "matched to y" since it is obtained from the unit impulse response of output y) is,

$$z_y(t) = \frac{\sigma_{h_z}}{2\pi} \int_{-\infty}^{\infty} X_z^*(\omega) X_y(\omega)\, e^{i\omega(t - t_o)}\, d\omega, \tag{9}$$

where σ_{h_z} is the RMS of the unit impulse response of output z, and $X_z(\omega)$ is the Fourier transform of the excitation, $x_z(t)$, matched to output z. Responses to $x_z(t)$ are constructed in a similar fashion.

The response of a particular output to any excitation other than its matched excitation will never exceed the maximum response to the matched excitation. So,

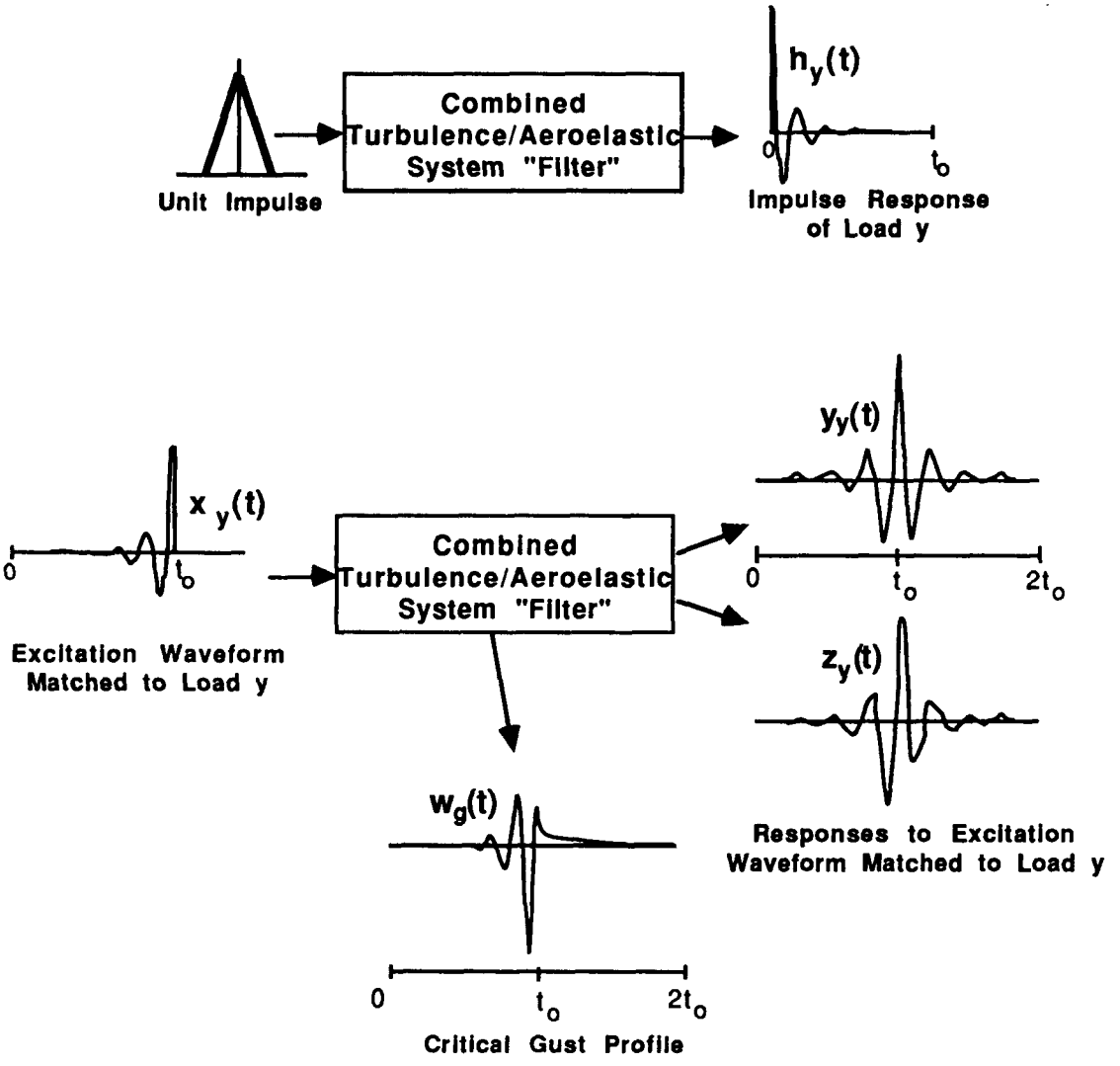

Figure 3. Application of Matched Filter Theory to Computing Time-Correlated Gust Loads

$$\left|y_z(t)\right| \le \left|y_y(t)\right|_{max} = \sigma_{h_y}, \tag{10}$$

and,

$$\left|z_y(t)\right| \le \left|z_z(t)\right|_{max} = \sigma_{h_z}. \tag{11}$$

Example Calculations of Time-Correlated Gust Loads Using Matched Filter Theory Approach

Example calculations of time-correlated gust loads using the MFT approach are shown in Figure 4, taken from Reference 2. The calculations were performed for a model of the NASA DAST ARW-2 vehicle in one-dimensional, random, vertical turbulence with a von Karman power spectrum with unit RMS gust velocity. In the aeroelastic model, 8 flexible modes are present, as well as plunge and pitch. The excitation used for these calculations was matched to the wing root bending moment. The figure shows bending and torsion moments at the wing root and bending moment at a station near the wing tip. Also shown is the critical gust profile obtained as an intermediate step in the procedure. The lag time, t_o (see Eqns. 6a and b), chosen at a point where the magnitude of the unit impulse response of the root bending moment has decayed to a small fraction of its largest magnitude, is 10 seconds. The root bending moment response to the matched excitation is maximum at this point. The other two responses are correlated in time with the "matched" root bending moment response. They are not maximum at t = 10 seconds, although the resolution in the figure does not permit this to be visible. Also, the "matched" root bending moment response is symmetric about the t = 10 second point whereas the other two time-correlated responses are not. The similarity between these plots and auto- and cross-correlation functions of RPT led the authors of Ref. 2 to establish a duality between MFT and RPT approaches to calculating time-correlated gust loads.

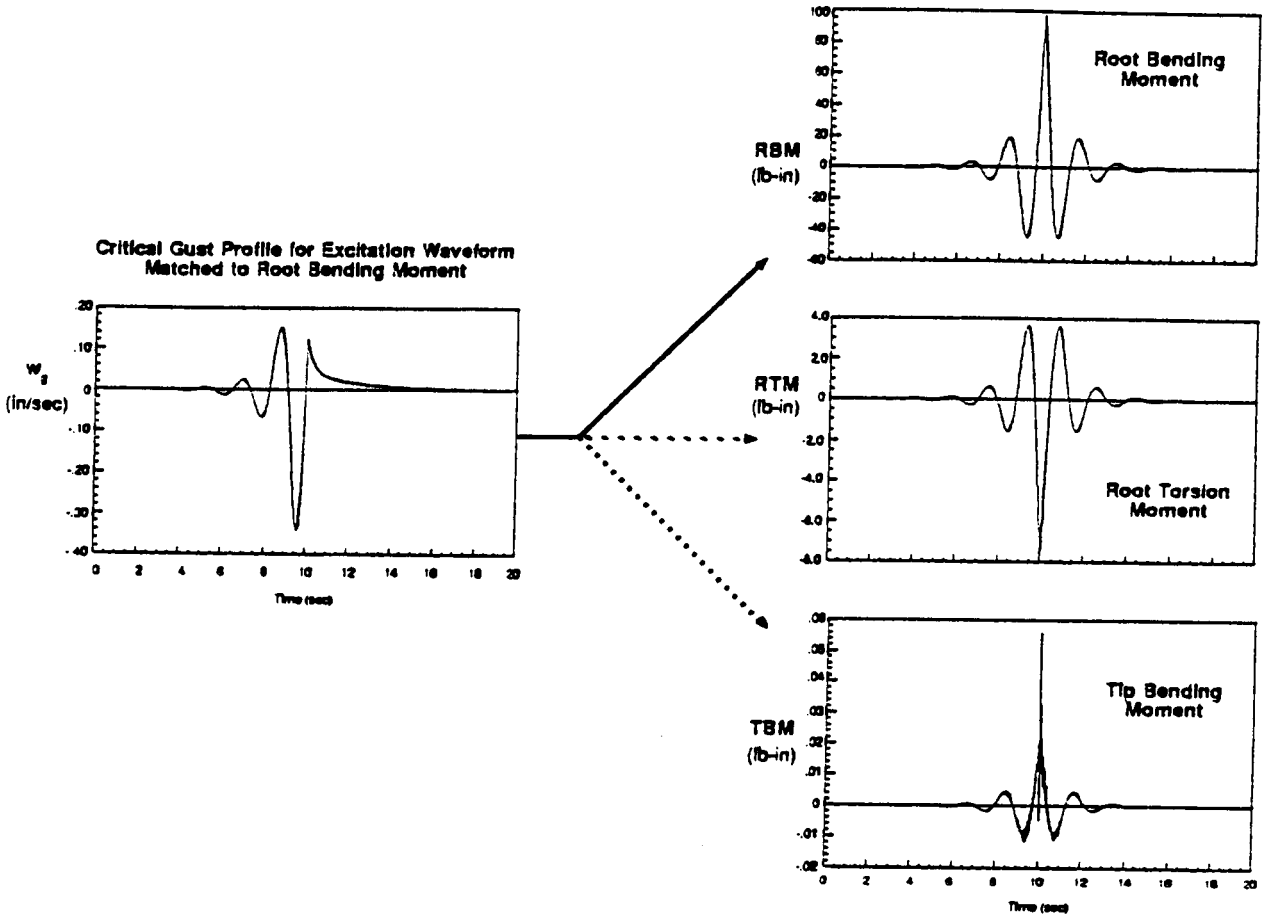

Figure 4. Example Calculations Using Matched Filter Theory Approach (from Ref. 2)

Duality Between Matched Filter and Random Process Theories

The duality between MFT and RPT can be seen analytically by substituting the Fourier transforms of the matched excitation waveforms as expressed in Eqn. 6b (recalling that the constant K is set equal to the RMS of the corresponding unit impulse response) into the expressions for the responses of the system to the waveforms as written in Eqns. 7 and 9. The results are

$$y_y(t) = \frac{1}{\sigma_{h_y}}\left[\frac{1}{2\pi}\int_{-\infty}^{\infty} H_y(\omega)H_y^*(\omega)\, e^{i\omega(t - t_o)}\, d\omega \right], \tag{12}$$

and

$$z_y(t) = \frac{1}{\sigma_{h_y}}\left[\frac{1}{2\pi}\int_{-\infty}^{\infty} H_z(\omega)H_y^*(\omega)\, e^{i\omega(t - t_o)}\, d\omega \right]. \tag{13}$$

The product $H_y(\omega)H_y^*(\omega)$ is the auto-PSD function for the response of output y and the product $H_z(\omega)H_y^*(\omega)$ is the cross-PSD function for the responses of outputs z and y. Thus the terms in the brackets in Eqns. 12 and 13 are, respectively, the auto- and cross-correlation functions, $R_{yy}(t - t_o)$ and $R_{zy}(t - t_o)$. The responses can then be written,

$$y_y(t) = \frac{1}{\sigma_{h_y}} R_{yy}(t - t_o)\,, \tag{14}$$

and

$$z_y(t) = \frac{1}{\sigma_{h_y}} R_{zy}(t - t_o)\,. \tag{15}$$

Further, the maximum value of R_{yy} at $t = t_o$ is $\sigma_{h_y}^2$, and thus $\left|y_y(t)\right|_{max}$ is σ_{h_y}, which is in agreement with Eqn. 8.

The utility of this duality is that these responses are obtained by calculating inverse Fourier transforms of the PSD functions of the combined turbulence/aeroelastic system without constructing representative frequency response functions, as required in the MFT approach. As stated in Ref. 2, " Thus RPT, normally employed to determine the statistical properties of random processes, may also be employed to obtain certain deterministic responses provided that they are interpreted as responses to matched excitation waveforms as described by MFT." Figure 5, again taken from Ref. 2, shows comparisons of calculations of time-correlated gust loads by the two methods. The slight differences are attributed to computational error. In the remainder of this report, references to results obtained from the MFT approach shall be understood to mean that the results are also obtainable from the RPT approach as well.

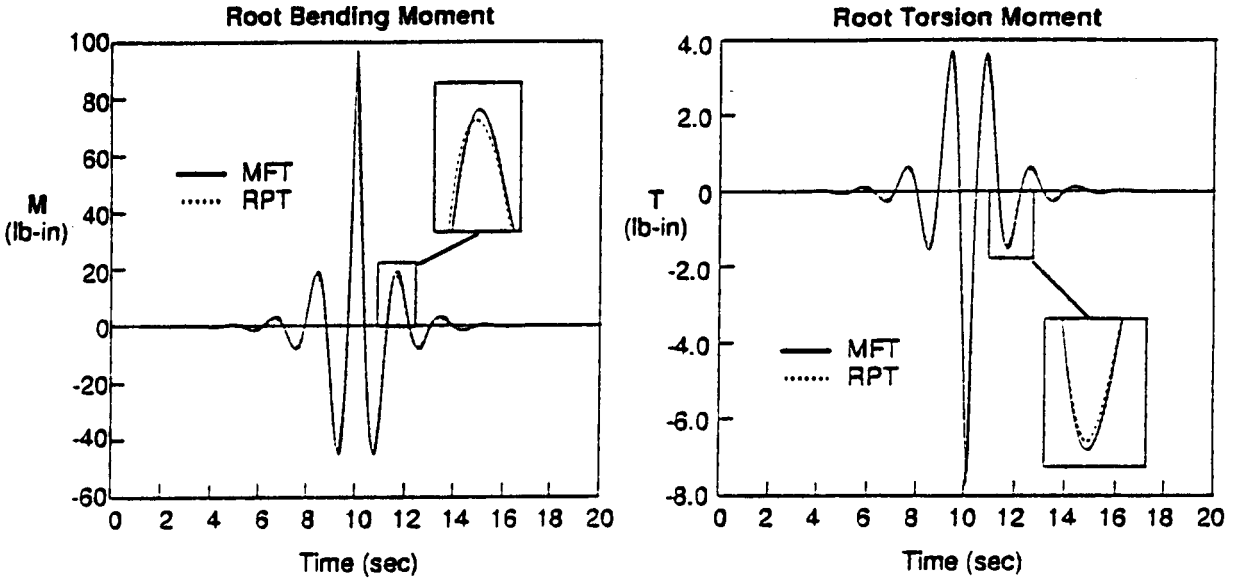

Figure 5. Comparison of Time-Correlated Gust Load Calculations by MFT and RPT Approaches (from Ref. 2)

RELATIONSHIP BETWEEN MFT APPROACH AND PHASED DESIGN LOADS ANALYSIS

Theoretical Basis

Let the response of output z to the excitation matched to y, Eqn. 15, be normalized by the maximum possible response of z (Eqn. 11), σ_{h_z}. This gives a general correlation coefficient that is a function of time,

$$\frac{z_y(t)}{\sigma_{h_z}} = \frac{R_{zy}(\tau)}{\sigma_{h_z}\sigma_{h_y}} = \rho_{zy}(\tau)\,, \tag{16}$$

where $\tau = t - t_o$. The frequency response function, $H_y(\omega)$, of the output y of the combined turbulence/aeroelastic system filter is a combination of a turbulence frequency response function, $G(\omega)$, and the aeroelastic response function, $\overline{H}_y(\omega)$. Thus

$$H_y(\omega) = G(\omega)\overline{H}_y(\omega), \tag{17}$$

and $G(\omega)G^*(\omega) = \Phi_g(\omega)$, which is the turbulence PSD (the squared magnitude of the turbulence frequency response function). Multiplying Eqn. 2 by $\sigma_g{}^2$, and evaluating the integral,

$$\sigma_{h_y}^2 = \sigma_g^2\,\overline{A}_y{}^2. \tag{18}$$

Analogous expressions are true for output z. Substituting Eqns. 17 and 18 (and the analogous equations for output z) into Eqn. 13 yields, using Eqn. 16 above,

$$\rho_{zy}(\tau) = \frac{1}{2\pi}\int_{-\infty}^{\infty}\frac{\left(\Phi_g(\omega)/\sigma_g^2\right)}{\overline{A}_z\,\overline{A}_y}\left[\,\overline{H}_z(\omega)\overline{H}_y^*(\omega)\,e^{\,i\omega\tau}\right]d\omega. \tag{19}$$

In terms of Eqn. 9,

$$\rho_{zy}(\tau) = \frac{1}{2\pi}\int_{-\infty}^{\infty} X_z^*(\omega)X_y(\omega)\,e^{\,i\omega\tau}\,d\omega. \tag{20}$$

Note that when $\tau = 0$ ($t = t_o$), Eqn. 19 becomes identical to Eqn. 5. Thus,

$$\rho_{zy}(0) = \rho_{zy}\,. \tag{21}$$

Similarly,

$$\frac{y_y(t)}{\sigma_{h_y}} = \frac{R_{yy}(\tau)}{\sigma_{h_y}^2} = \rho_{yy}(\tau)\,, \tag{22}$$

and,

$$\rho_{yy}(0) = 1. \tag{23}$$

The general correlation coefficients of Eqns. 16 and 22, which can now be interpreted as normalized responses to the excitation matched to y, may be plotted as parametric functions

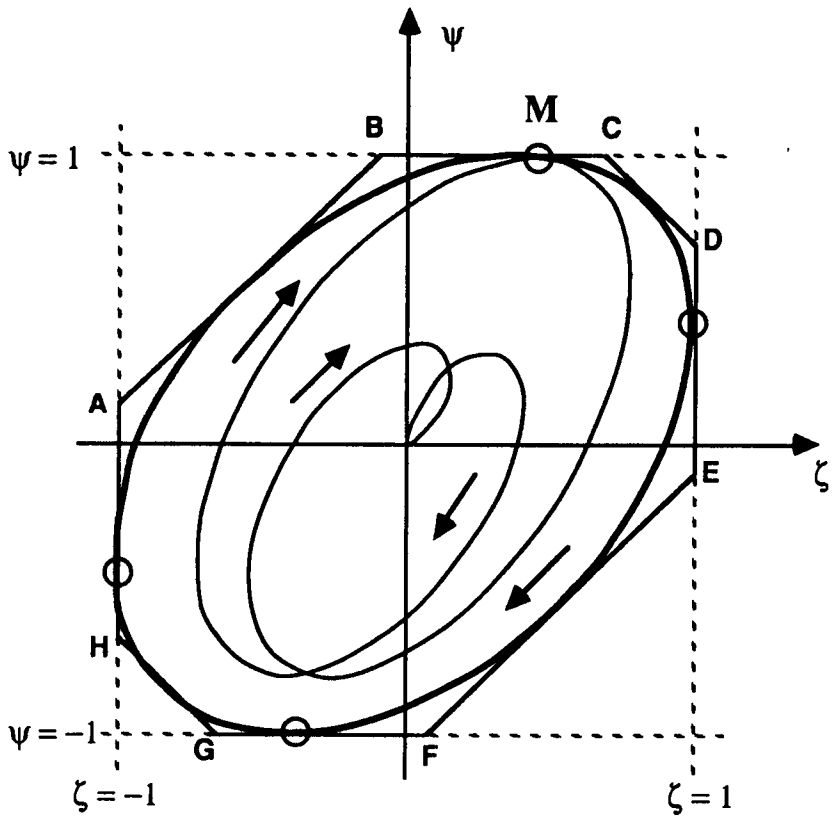

Figure 6. Normalized Design Ellipse With Parametric Load Plot

of time with the normalized design ellipse. Figure 6 shows, in a general way, how the plot would appear. The plot grows from zero, oscillating to a point M (at $t = t_o$, $\tau = 0$) where it is tangent to the ellipse. It then decays back toward zero. The (ψ,ζ) coordinates of point M are $(1, \rho_{zy})$, and correspond to the design value of y and the "phased" value of z.

Example Calculations

The ellipse and parametric load plot shown earlier in Fig. 6 were simplified for clarity and were purely hypothetical. In practice, such a wide ellipse and spiraling load plot would be indicative of loads that were not very highly correlated and had a limited range of frequency content. In the following figures are shown normalized design ellipses and normalized load time histories, some of which correspond to the examples presented previously in Fig. 4. Figure 7 shows wing root torsion and bending moment responses to the excitation matched to wing root bending moment (i.e., a combination of the responses depicted in the top two boxes at the right of Fig. 4). The value of the correlated response (torsion) is -0.843 when the matched response (bending) is unity. Thus, the value of the correlation coefficient used to construct the ellipse is, then, -0.843.

Although not clear in the figure, the load plot starts at zero and oscillates with increasing amplitude nearly on a straight line, becoming tangent to the ellipse, then decaying back toward zero. The frequency with which the plot oscillates corresponds to the short period mode and is readily visible in the major oscillations of the response shown in Fig. 4. There is a high degree of correlation (ρ = -0.843) between the loads since both respond strongly to the short period content of the excitation, which is matched to root bending. Torsion, however, is less responsive to the short period frequency, and more responsive to higher frequencies than is the bending. Thus one observes the slightly lower magnitude (0.843) of the torsion load and lateral deviations (in the direction of the torsion axis) from a straight line in the load plot.

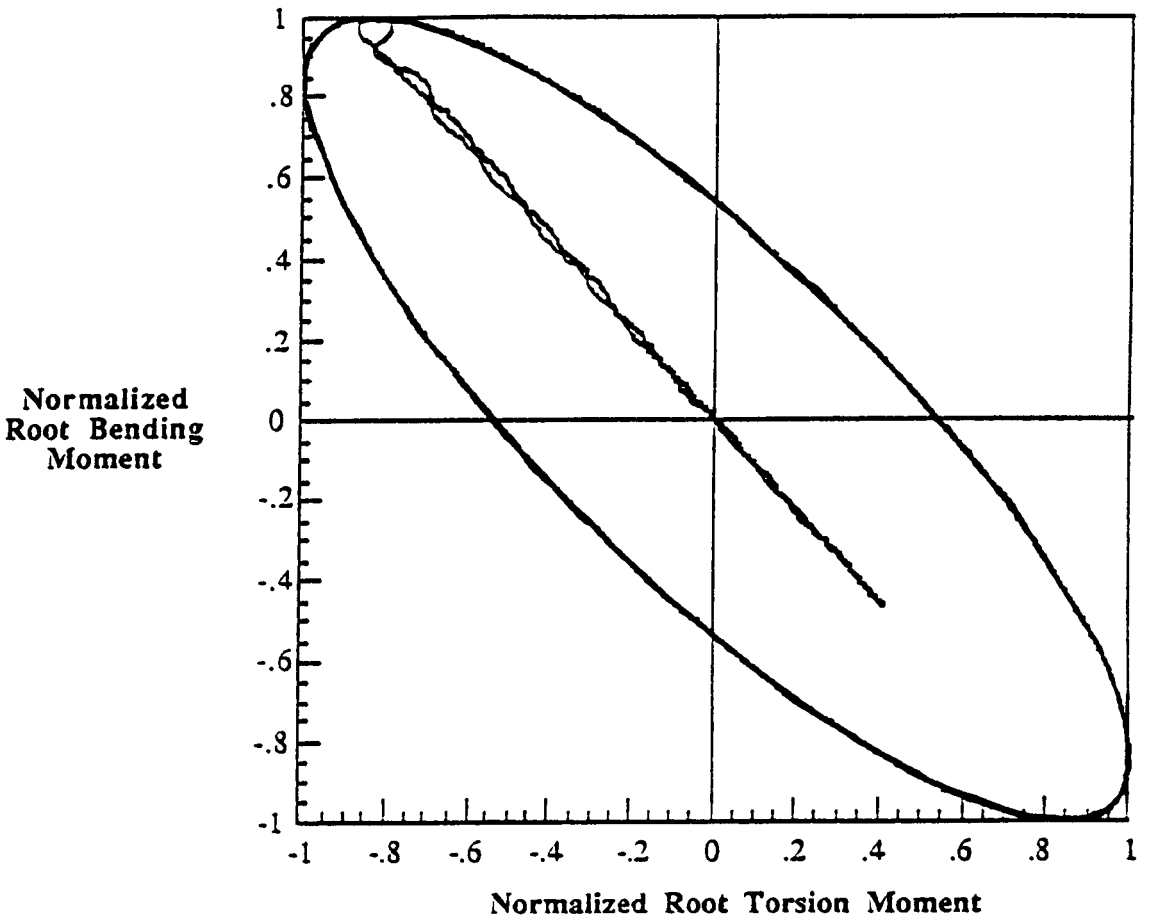

Figure 7. Normalized Design Ellipse With Normalized Parametric Load Plot: Wing Root Bending and Torsion Moment Responses to Excitation Matched to Root Bending Moment

Example Calculations (cont.)

Figure 8 shows wing root torsion and bending moment responses to the excitation matched to wing root torsion moment. As in Fig. 7, the value of the correlated response (bending) is -0.843 when the matched response (torsion) is unity. Again, there is a high degree of correlation between the loads in the lower frequency, short-period-dominated response. The deviations from a straight line resulting from the higher frequency, elastic-mode-dominated portion of the responses are more pronounced than in Fig.7. This occurs because the excitation, matched to torsion in this case, has more higher frequency content than the excitation matched to bending. Thus, the torsion responds more readily and reaches its maximum value.

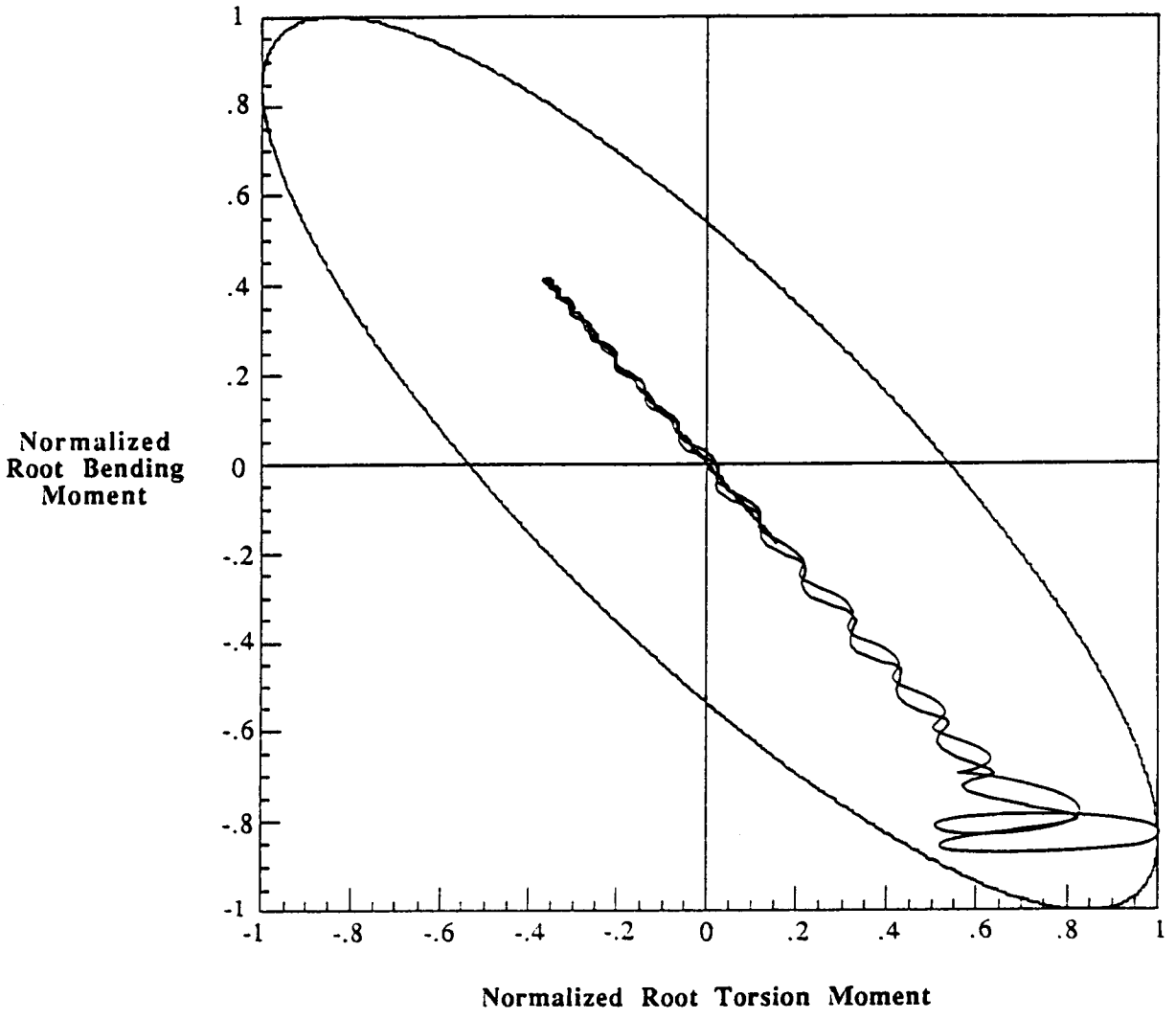

Figure 8. Normalized Design Ellipse With Normalized Parametric Load Plot: Wing Root Bending and Torsion Moment Responses to Excitation Matched to Root Torsion Moment

Example Calculations (cont.)

Figure 9 shows the parametric load responses for wing root bending moment and wing tip bending moment for the excitation matched to root bending moment (i.e. a combination of the responses depicted in the top and bottom boxes at the right of Fig. 4). The correlation coefficient for constructing the ellipse in this case is 0.103. This relatively low value results in the ellipse's being much closer to a circle than in the previous case. It is somewhat surprising, since the load plot is nearly a straight line. However, the excitation producing these responses is that which is matched to root bending, and root bending is more responsive to the short period frequency than is tip bending moment. So, even though the major oscillations of the load plot are at the short period frequency, the relatively unresponsive tip bending moment does not reach anywhere near its potential maximum, resulting in the low value of the correlation coefficient. The drastic effects of an excitation matched to an output *not* highly responsive to the short period frequency can be seen in the next figure.

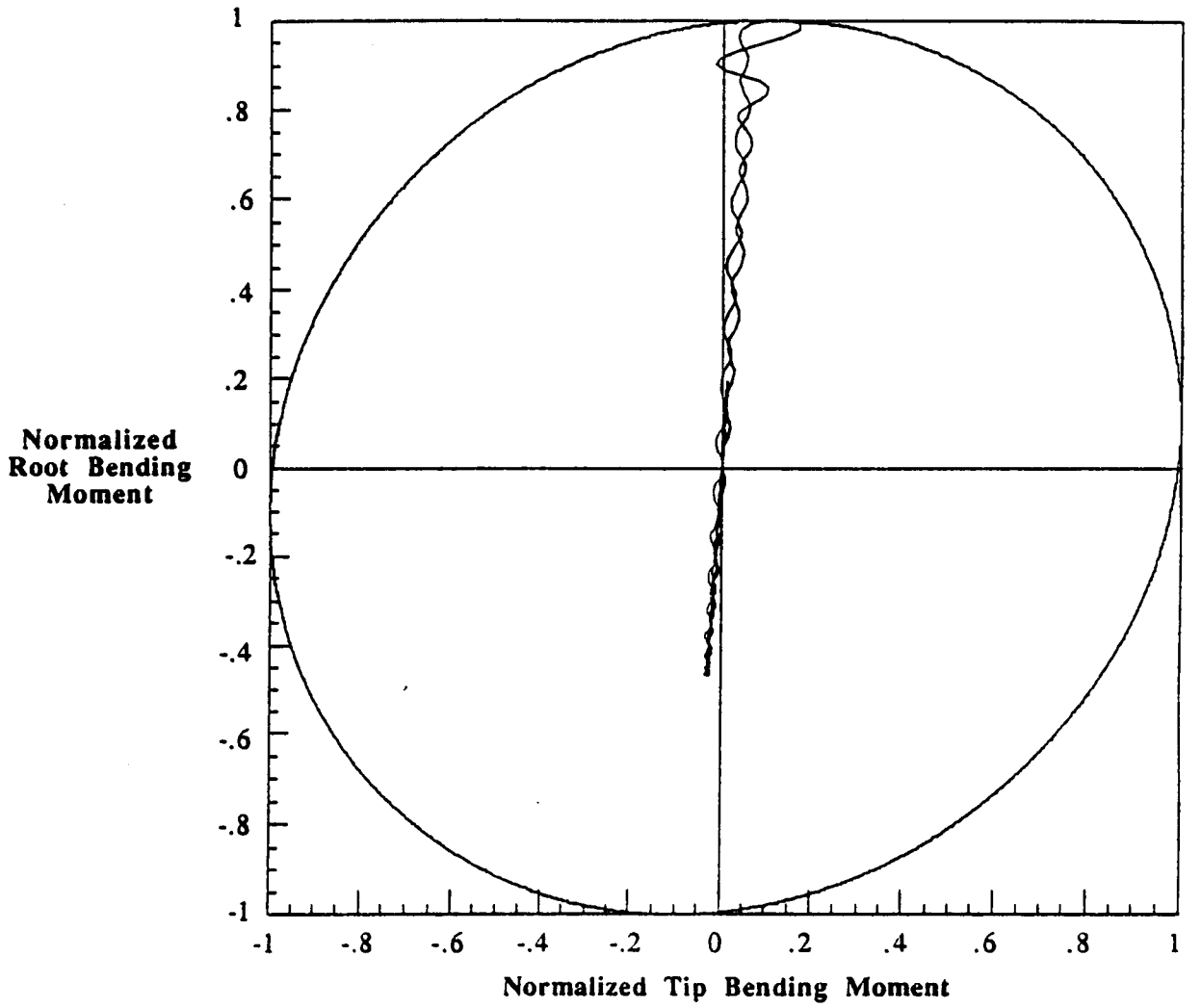

Figure 9. Normalized Design Ellipse With Normalized Parametric Load Plot: Wing Root Bending and Wing Tip Bending Moment Responses to Excitation Matched to Root Bending Moment

Example Calculations (concl.)

Figure 10 shows parametric load responses for root and tip bending moments resulting from the excitation matched to tip bending moment. The lower frequency oscillations are still alligned toward the root bending moment axis as in all the other cases. However, the degree of lateral deviations (along the tip bending moment axis) is quite pronounced. The tip bending moment is clearly more responsive to the higher frequency content of its matched excitation than to the lower frequency content (short period) of the excitation matched to root bending.

The example plots show that some of the loads may appear highly correlated (i.e. have correlation coefficients near ± 1 and their parametric plots falling nearly on a straight line) in the lower frequency, short-period-dominated components if the excitation is matched to the output quantity most responsive to the short period frequency. For cases in which the excitation is matched to an output that is *less* responsive to the short period frequency, such as in Figs. 8 and 10, the parametric plots appear less correlated, displaying larger lateral deviations from a straight line. However, the correlation coefficients need not be very low (and, thus, the associated ellipses need not be wide and near-circular) even if the lateral deviations are rather sizeable, as in Fig. 8. This raises the question of whether or not it is possible for any parametric load plot to extend outside the associated design ellipse. It is possible to prove, using Eqns. 10 and 11, that the plots cannot extend beyond the square that bounds the normalized design ellipse. However, the authors cannot, as yet, offer a proof that the design ellipse bounds the parametric load plot. The limited results presented in this report suggest that wide oscillations in load plots are not necessarily accompanied by very low correlation coefficients (and thus wide and near-circular ellipses). Nonetheless, the ellipses appear to always be sufficiently wide to accommodate the load oscillations. The question needs resolution because if the parametric load plots can exceed the ellipse, then the use of the equiprobable loads design ellipse is not always a conservative design practice.

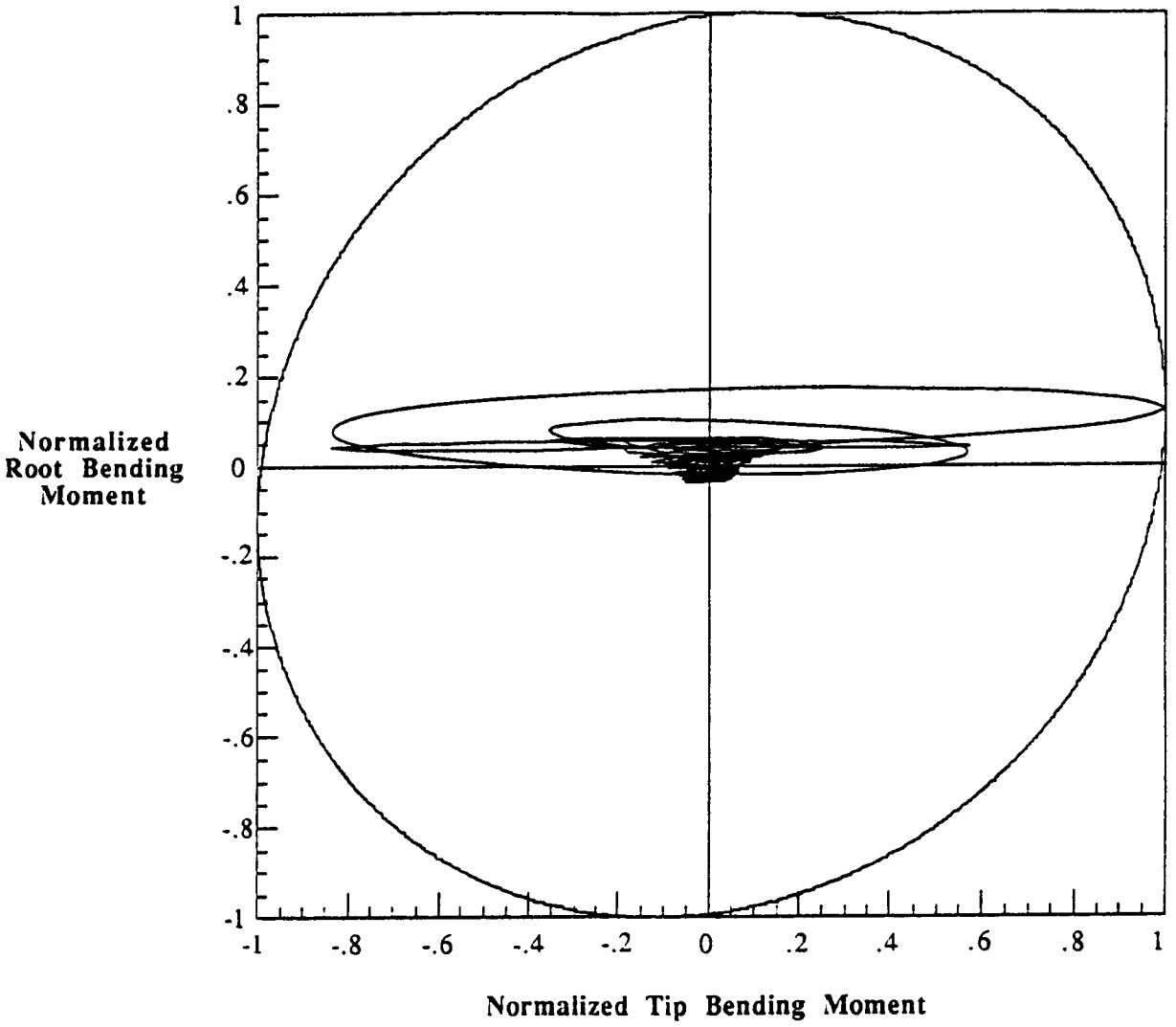

Figure 10. Normalized Design Ellipse With Normalized Parametric Load Plot: Wing Root Bending and Wing Tip Bending Moment Responses to Excitation Matched to Tip Bending Moment

CONCLUDING REMARKS

This report has given a theoretical basis and example calculations that demonstrate the relationship between the Matched Filter Theory approach to the calculation of time-correlated gust loads and Phased Design Loads Analysis in common use in the aerospace industry. The relationship depends upon the duality between Matched Filter Theory and Random Process Theory and upon the fact that Random Process Theory is used in Phased Design Loads Analysis in determining an equiprobable loads design ellipse. It was then shown that the time histories of two time-correlated gust load responses, determined using the Matched Filter Theory approach, can be plotted as parametric functions of time and that the resulting plot, when superposed upon the design ellipse corresponding to the two loads, is tangent to that ellipse. The point of tangency is the point at which the response to which the excitation is "matched" (in the sense of Matched Filter Theory) reaches its maximum value. This value is the design value for that load, as used in Phased Design Loads Analysis. If the loads are normalized as outlined in the report, this maximum value is unity and the value of the time-correlated response of the second load, corresponding to the "phased" value, is equal to the correlation coefficient used to construct the design ellipse. The question is raised of whether or not it is possible for a parametric load plot to extend outside the associated design ellipse. If so, then the use of the equiprobable loads design ellipse will not be a conservative design practice in some circumstances.

REFERENCES

1. Jones, J. G.: Statistical Discrete Gust Theory for Aircraft Loads. RAE Technical Report 73167, 1973.

2. Pototzky, Anthony S.; Zeiler, Thomas A.; and Perry III, Boyd: Time-Correlated Gust Loads Using Matched Filter Theory and Random Process Theory - A New Way of Looking at Things. AIAA Paper No. 89 - 1374CP, *Proceedings of the AIAA/ASME/ASCE/AHS 30th Structures, Structural Dynamics and Materials Conference*, April 3 - 5, 1989.

3. Fuller, J. R.; Richmond, L. D.; Larkins, P. C.; and Russel, S. W.: Contributions to the Development of a Power-Spectral Gust Design Procedure for Civil Aircraft. FAA - ADS - 54, Jan. 1966.

4. Moon, Richard N.: A Summary of Methods for Establishing Airframe Design Loads from Continuous Gust Design Criteria. Presented at the 65th AGARD Structures and Materials Panel, Turkey, October 4 - 9, 1987.

5. Noback, R.: How to Generate Equal Probability Design Load Conditions. NLR TR 86060 U, 1985.

6. Carlson, A. Bruce: *Communication Systems*, McGraw - Hill Book Company, New York, 1968.

NASA
National Aeronautics and Space Administration

Report Documentation Page

1. Report No.	2. Government Accession No.	3. Recipient's Catalog No.
NASA CR-181802		

4. Title and Subtitle	5. Report Date
On the Relationship Between Matched Filter Theory as Applied to Gust Loads and Phased Design Loads Analysis	April 1989
	6. Performing Organization Code

7. Author(s)	8. Performing Organization Report No.
Thomas A. Zeiler Anthony S. Pototzky	
	10. Work Unit No. 505-63-21-04

9. Performing Organization Name and Address	11. Contract or Grant No.
Planning Research Corporation Aerospace Technologies Division 303 Butler Farm Road, Suite 100 Hampton, Virginia 23666	NAS1-18000
	13. Type of Report and Period Covered Contractor Report

12. Sponsoring Agency Name and Address	14. Sponsoring Agency Code
National Aeronautics and Space Administration Langley Research Center Hampton, Virginia 23665-5225	

15. Supplementary Notes

Langley Technical Monitor: Thomas E. Noll

Presented at the 1989 Gust Specialists Meeting, Mobile, Alabama, April 6, 1989.

16. Abstract

This report gives a theoretical basis and example calculations that demonstrate the relationship between the Matched Filter Theory approach to the calculation of time-correlated gust loads and Phased Design Load Analysis in common use in the aerospace industry. The relationship depends upon the duality between Matched Filter Theory and Random Process Theory and upon the fact that Random Process Theory is used in Phased Design Loads Analysis in determining an equiprobable loads design ellipse. Extensive background information describing the relevant points of Phased Design Loads Analysis, calculating time-correlated gust loads with Matched Filter Theory, and the duality between Matched Filter Theory and Random Process Theory is given. It is then shown that the time histories of two time-correlated gust load responses, determined using the Matched Filter Theory approach, can be plotted as parametric functions of time and that the resulting plot, when superposed upon the design ellipse corresponding to the two loads, is tangent to the ellipse. The question is raised of whether or not it is possible for a parametric load plot to extend outside the associated design ellipse. If it is possible, then the use of the equiprobable loads design ellipse will not be a conservative design practice in some circumstances.

17. Key Words (Suggested by Author(s))	18. Distribution Statement
Time-Correlated Gust Loads Matched Filter Theory/Random Process Theory Duality Phased Design Loads Analysis Equiprobable Loads Design Ellipse	Unclassified - Unlimited Subject Category - 05

19. Security Classif. (of this report)	20. Security Classif. (of this page)	21. No. of pages	22. Price
Unclassified	Unclassified	26	A03